

Analysis of power parameters of the squirrel cage motor and LSPMS motor with U-shaped magnets

Abstract. The paper presents the special algorithm and software for the transient FE analysis of electromagnetic phenomena in a squirrel cage induction motor and in a line start permanent magnet synchronous motor. The presented algorithm and the elaborated specialized software for the finite element analysis of transients and steady states are used to determine the power parameters of the squirrel-cage induction motor as well as the Line Start Permanent Magnet Synchronous Motor (LSPMSM). The nonlinearity of the magnetic circuit, the movement of the rotor and the skewed slots have been taken into account. The results of computations have been compared with measurements. The conclusions from the comparison of calculation results with the results of measurements were presented. (*Analiza parametrów energetycznych silnika indukcyjnego klatkowego i silnika synchronicznego z magnesami w kształcie litery U o rozruchu bezpośrednim*).

Streszczenie. W artykule przedstawiono model polowy oraz opracowane na jego podstawie algorytm oraz oprogramowanie do analizy procesu rozruchu i ustalonych stanów pracy silnika indukcyjnego klatkowego oraz silnika synchronicznego magnetoelektrycznego przystosowanego do rozruchu bezpośredniego. W rozważaniach uwzględniono nieliniowość obwodu magnetycznego, ruch wirnika oraz skoszenie żłobków wirnika w silniku indukcyjnym. Obliczenia związane z uwzględnieniem skosu rdzenia stojana wykonano przy zastosowaniu modelu quasi-trójwymiarowego. Zaprezentowano wybrane rezultaty badań symulacyjnych i laboratoryjnych. Przedstawiono wnioski wynikające z porównania wyników obliczeń z rezultatami pomiarów.

Keywords: squirrel cage motor, LSPMS motor, finite element analysis, field-circuit model

Słowa kluczowe: silnik indukcyjny klatkowy, silnik synchroniczny magnetoelektryczny o rozruchu bezpośrednim, metoda elementów skończonych, model polowo-obwodowy

Introduction

Induction motors still used in electric drives are being increasingly replaced by synchronous motors with permanent magnets (PMSM). This is due to the reduction of operating costs of the latter ones, resulting from the increase in the efficiency and power factor while reducing their dimensions in comparison with conventional induction motors of the same power. Many interesting PMSM constructions have been described in the literature. Motors with segmented magnets placed on the rotor surface are presented in papers [10, 12]. In order to reduce time and production costs, it is proposed e.g. to make motor components of powder material in one technological process [8, 14].

The main disadvantage of the PMSM is the necessity to make use of electronic power converter systems to make them start. This significantly increases the costs of the entire drive system. In order to avoid this drawback, intensive works on the LSPMSM are carried out in many scientific research centers [7, 9, 11].

In this paper, the authors present the results of simulation and laboratory tests of functional motor parameters, such as the efficiency, power factor and power output. A squirrel cage motor and the LSPMSM with the same linear dimensions were examined. The calculations have been performed with the use of computer software elaborated by the authors. The software has been prepared and is successfully applied in the design of special squirrel cage motors [2], e.g. motors working in cryogenic conditions [2].

Examined motors

The Sg 100L-4B type, three-phase squirrel cage induction motor with a power of $P_N=3$ kW (Fig. 1a) and the prototype of the designed LSPMSM motor (Fig.1b) were examined. The same stator was used in both motors (Fig.2b). The LSPMSM rotor included the starter squirrel cage with 28 aluminum round rods and neodymium magnets arranged in the U shape – Fig. 2.

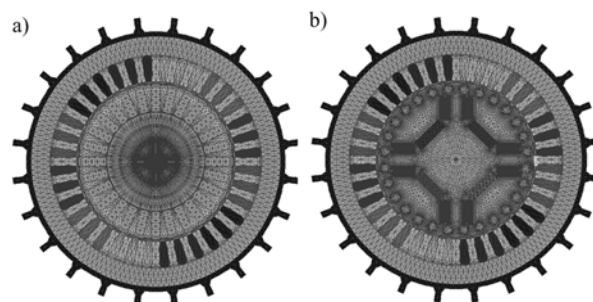


Fig.1. The structures of rotors: a) IM, b) LSPMSM

In the design process of new constructions of the LSPMSM, it is beneficial to utilize components of the classic asynchronous motor. The key reason is the manufacturing costs reduction, by keeping motor sizes and their interfaces in the range of produced series of induction machines. The components that can be easily taken from induction machines (IM) are i.e. terminal boxes, stator cores, housings, bearing and cooling systems. In order to reduce the manufacturing costs of the LSPMS motor the prototype of this synchronous motor has been based on the stator of the considered squirrel-cage induction motor [3].

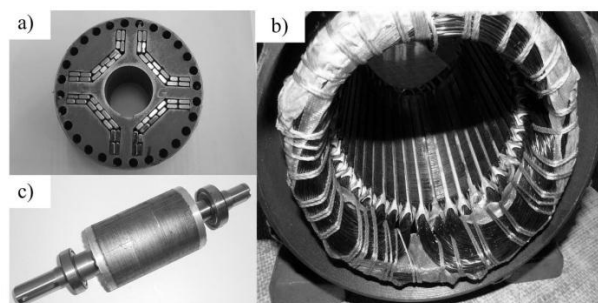


Fig.2. Prototype of designed rotor of LSPMSM (a) and (c), stator of the three phase induction motor, type Sg 100L-4B (b)

The use of the same stator core makes a comparative analysis of energy parameters in both motors easier. In order to achieve the optimal utilization of the magnetic circuit the excitation system using a rare earth permanent magnet has been designed [14]. In the analysis of the electromagnetic circuit of the motor, the influence of design variables such as permanent magnet properties, cage shape, magnet arrangement and the main dimensions of the motor subcomponents on motor parameters have been studied. The design and the optimization process have been based on the circuit, field and field circuit models. To avoid saturation of the stator it has been assumed that amplitude of the first harmonic of the flux density in the air-gap (excited by PM's) should be close to the value calculated for the base machine. The view of the designed rotor prototype has been shown in Fig. 2c. In order to reduce the costs of the prototype the small size stock available NdFeB magnets have been utilized.

Finite element formulation

The mathematical model of electromagnetic phenomena in a squirrel cage motor as well as a LSPMS motor include the equations of the electromagnetic field and the mechanical equilibrium equations of the considered electromechanical system. In order to describe the electromagnetic field the magnetic vector potential \mathbf{A} and the electric potential V have been applied [5]. In this case, the equation describing the transient electromagnetic field in the motor can be expressed as [6].

$$(1) \quad \nabla \times \left(\frac{1}{\mu} \nabla \times \mathbf{A} \right) = \mathbf{J} + \mathbf{J}_m,$$

$$(2a) \quad \mathbf{J} = -\sigma(d\mathbf{A}/dt + \nabla V),$$

$$(2b) \quad \mathbf{J}_m = \nabla \times \mathbf{M},$$

where μ is the magnetic permeability, \mathbf{J} is the current density vector and σ is the conductivity of the medium, \mathbf{J}_m is the current density vector representing the magnetization of the permanent magnet, \mathbf{M} is the magnetization vector in the region with permanent magnets.

In our considerations, it has been assumed that the magnetic properties of magnetic soft materials and permanent magnets are described by equation (3) and (4) respectively.

$$(3) \quad \mathbf{B} = \mu(\mathbf{H}),$$

$$(4) \quad \mathbf{B} = \mu_0(\mathbf{H} + \mathbf{M}),$$

where \mathbf{B} is the vector of magnetic flux density, \mathbf{H} is the magnetic field strength vector, μ_0 is the magnetic permeability of the vacuum.

In general, the transient electromagnetic field in the electrical machines is voltage-excited. This means that the phase currents in the windings are not known in advance, i.e., prior to electromagnetic field calculation [13]. Therefore, it is necessary to consider the equations of the electric circuit of the device. The set of independent loop equations may be written as:

$$(5) \quad \mathbf{u} = \mathbf{R}\mathbf{i} + \frac{d}{dt}\mathbf{\Psi},$$

where \mathbf{u} is the vector of supply voltages, \mathbf{i} is the vector of loop currents, \mathbf{R} is the matrix of loop resistances, $\mathbf{\Psi}$ is the flux linkage vector. The vector $\mathbf{\Psi}$ is calculated by means of the field model.

The equations of field-circuit model are coupled through the electromagnetic torque T to the equation of motion

$$(6) \quad J \frac{d^2 \alpha}{dt^2} + T_L + T_f = T,$$

where J is the moment of inertia, α is the angular position of the rotor, T_L is the load torque, T_f is the resistive torque produced in the motor bearings and fan.

The electromagnetic torque T in equation (6) is calculated on the basis of the magnetic field distribution [4].

In order to solve non-linear equations (1) – (6) only approximate methods can be applied, based on the discretization of space and time [5].

In the paper, the problem was considered as a two-dimensional one, and so-called field-circuit methods were used in the analysis of squirrel cage and LSPMS motors [4]. In order to represent the skew of the rotor slots, the machine was cut into w disks (sections) along the z -axis parallel to the shaft [1]. Each section concerns the different position of the rotor with respect to the stator. The magnetic coupling of the disks is neglected. The stator winding of the machine is composed of coils with thin conductors connected in series. In the rotor, the squirrel-cage winding is used. In our model, the windings are segmented into elementary conductors associated with disks. The electric connections of the stator and rotor windings sections are taken into account. They are represented by circuit equations [4]. Moreover the resistances and inductances of the stator winding end-turns and the rotor end-rings are considered. Detailed description of the multi-slice model of the rotor was presented in the papers [1, 2].

The time discretization leads to the following system of non-linear algebraic matrix equations

$$(7) \quad \begin{bmatrix} \mathbf{S}_w^n + \mathbf{G}_w(\mathbf{I} - \mathbf{C}_w)\Delta t^{-1} & -\mathbf{z}_w \\ -[\mathbf{z}_w^T] & -(\mathbf{R}\Delta t + \mathbf{L}) \end{bmatrix} \begin{bmatrix} \mathbf{\Phi}_w^n \\ \mathbf{i}^n \end{bmatrix} = \begin{bmatrix} \mathbf{M}_{mw}^n \\ -\Delta t \mathbf{U}^n \end{bmatrix} + \begin{bmatrix} \mathbf{G}_w(\mathbf{I} - \mathbf{C}_w)\Delta t^{-1} & \mathbf{0} \\ -\mathbf{z}_w^T & -\mathbf{L} \end{bmatrix} \begin{bmatrix} \mathbf{\Phi}_w^{n-1} \\ \mathbf{i}^{n-1} \end{bmatrix},$$

where: n denotes the number of time-steps; w is the number of rotor disk (sections) along the z axis parallel to the shaft (for the LSPMSM w is equal 1); Δt is the time-step length; \mathbf{M}_{mw} is the vector of magnetomotive force in regions with the permanent magnets (for IM elements of matrix \mathbf{M}_{mw} are equal to 0), \mathbf{S}_w^n , \mathbf{G}_w , \mathbf{C}_w , \mathbf{z}_w are the coefficients submatrices for disks; \mathbf{L} is the matrix of end-turns inductances.

In order to approximate the time-derivatives in equation (6) describing the motion of the rotors, an explicit formula has been used

$$(8) \quad J(\alpha_{n+1} - 2\alpha_n + \alpha_{n-1})/(\Delta t)^2 = T - T_L - T_f.$$

The angular velocity ω of the rotor is determined by following the formula

$$(9) \quad \omega(t_n + 0.5\Delta t) = (\alpha_{n+1} - \alpha_n)/\Delta t.$$

The movement of the rotor is simulated by means of the moving band method. In the elaborated algorithm and computer software equations (7) and (8) are solved with the aid of the Newton-Raphson iterative procedure. The electromagnetic torque was calculated using the FE representation of the Maxwell stress tensor formula. The formula was obtained by the analysis of the virtual displacement corresponding to the moving band method.

Results

On the basis of the presented algorithm for solving equations within the field-circuit model, the computer program for the simulation of electromagnetic phenomena in the full-scale model of squirrel-cage motor and the LSPMS motor was elaborated. This program has been developed in the Borland Delphi environment. It allows automatic generation of mesh of the area with the user selected software parameters such as: number of pole pairs, the number of stator and rotor windings, single or dual-layer winding, fractional slot winding, winding connection. Developed procedures used in special computer software allow you to choose different shapes of motor slots. For the purpose of the program the base of magnetic soft and hard materials has been developed. The analysis of the phenomena in the considered motors can be carried out without taking into account as well as considering the skewed rotor slots. The program allows to carry out the calculations using a three-phase motor power system sinusoidal voltage as well as distorted voltages. The results of the calculation can be visualized as graphs, waveforms, electromagnetic field distribution, schedules and later saved as a file for further processing.

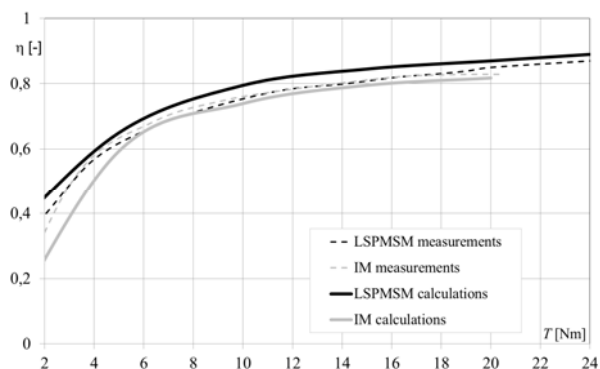


Fig.3. Efficiency as a function of load torque

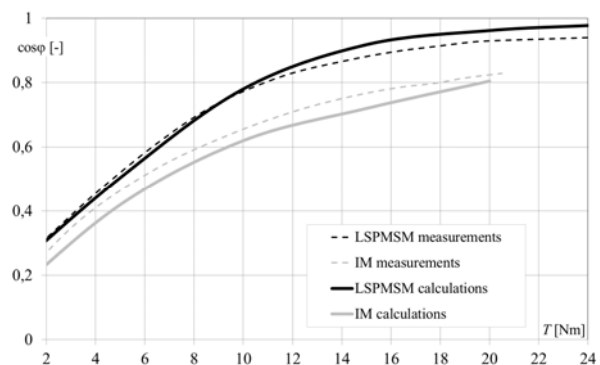


Fig.4. Power factor as a function of load torque

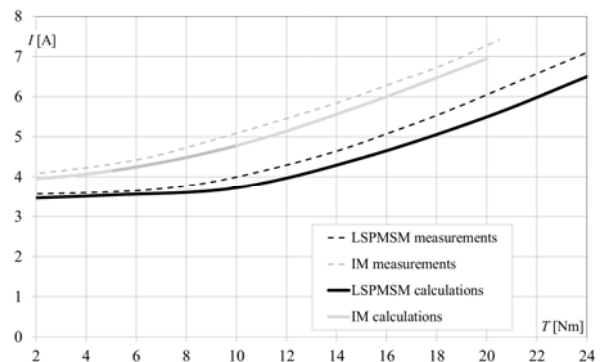


Fig.5. Current as a function of load torque

On the basis of the calculations the efficiency, the power factor and the line current as a function of the load torque were determined for the examined motors. The calculation results compared with the measurement results are listed in Fig.3-5. The obtained characteristics confirm the improvement of the LSPMSM operating parameters (the higher efficiency and power factor and lower current in stator windings for the same load) in comparison with the parameters of the induction motor with the same stator.

In order to compare the energy parameters of both motor constructions, the values of efficiency η , power factor $\cos\phi$, currents in stator winding I and power output P_u are summarized in Table 1. For the rated load torque $T = 20$ Nm, the current of the LSPMSM is by about 20% lower than that of the induction motor. It results from the lower power loss and makes possible to increase the load torque of the LSPMSM to $T = 24$ Nm. As a result, an increase of the power output of the LSPMSM by over 25% was obtained in comparison with that one of the induction motor. The power output increase is due to both the load torque increase and the rotational speed increase up to 1500 rpm.

Table 1. Selected functional parameters in steady state obtained during laboratory tests

| motor parameters | IM | LSPMSM | |
|------------------|-----------------|-----------------|-----------------|
| | $T=20\text{Nm}$ | $T=20\text{Nm}$ | $T=24\text{Nm}$ |
| η [%] | 0.81 | 0.86 | 0.88 |
| $\cos\phi$ [-] | 0.81 | 0.93 | 0.94 |
| I [A] | 7.2 | 6.0 | 7.1 |
| P_u [kW] | 3.0 | 3.1 | 3.8 |

Conclusions

After application of the rotor with the properly shaped magnetic circuit equipped with permanent magnets and the starter squirrel cage in the induction motor, it is possible to obtain a synchronous motor capable of self-starting, even under load. The effective parameters of the LSPMSM are better than those of the induction motor. The power factor and the efficiency of the motor with permanent magnets are significantly higher than those obtained from the induction motor. The effective current value of the LSPMSM in steady-state is also lower by approx. 20% than that of the induction motor for the same load of both machines. The results of simulation tests and measurements confirm that it would be advisable to implement this type of motor for the production and use. The usefulness of the software developed for the computer aided design of the cage induction motor and the LSPMS motor have been proven.

REFERENCES

- [1] Barański M., Demenko A., Łyskawiński W., Szeląg W., Finite element analysis of transient electromagnetic-thermal phenomena in a squirrel cage motor, *COMPEL*, 30 (2011), No. 3, 832 – 840
- [2] Barański M., Szeląg W., Finite element analysis of transient electromagnetic-thermal phenomena in a squirrel cage motor working at cryogenic temperature, *IET Science Measurement and Technology*, 6 (2012), No 5, 357 – 363
- [3] Barański M., Szeląg W., Jędryczka C., Mikołajewicz J., Łukaszewicz P., Analiza i badanie silnika synchronicznego o rozruchu bezpośrednim i magnesach w wirniku rozłożonych w kształcie litery U. *Przegląd Elektrotechniczny*, R. 89, Nr 2b/2013, 107-111
- [4] Demenko A., Movement simulation in finite element analysis of electric machine dynamics, *IEEE Transactions on Magnetics*, 32 (1996), No 3, 1553-1556
- [5] Driesen J., Coupled electromagnetic-thermal problems in electrical energy transducers, (2000), *Katholieke Universiteit Leuven*.

- [6] Driesen J., Belmans R. J. M., Hameyer K., Methodologies for Coupled Transient Electromagnetic-Thermal Finite-Element Modeling of Electrical Energy Transducers, *IEEE Transactions on Industry Applications*, 38 (2004), No 5, 1244-1250
- [7] Fei W., Luk K.P.C., Ma J., Shen J.X., Yang G., A high-performance line-start permanent magnet synchronous motor amended from a small industrial three-phase induction motor, *IEEE Transactions on Magnetics*, 45 (2009), No. 1, 4724-4727
- [8] Gwoździwicz M., Zawilak J., Influence of the rotor construction on the single-phase line start permanent magnet synchronous motor performances, *Przegląd Elektrotechniczny*, R.87, NR 11/2011, 135-138
- [9] Knight A.M., McClay C.I., The design of high-efficiency line-start motors, *IEEE Transactions on Industry Applications*, 36 (2000), No. 6, 1555-1562
- [10] May H., Palka R., Paplicki P., Szkolny S., Canders W.-R., Modified concept of permanent magnet excite synchronous machines with improved high-speed features, *Archives of Electrical Engineering*, 60 (2011), No. 4, 531-540
- [11] Miller T.J.E., Popescu M., Cossar C., McGilp M.I., Strappazon G., Trivillin N., Santarossa R., Line start permanent magnet motor: single-phase steady-state performance analysis, *IEEE Transactions on Industry Applications*, 40 (2004), No. 2, 516-525
- [12] Młot A., Korkosz M., Łukaniszyn M., Iron loss and eddy-current loss analysis in a low-power BLDC motor with magnet segmentation, *Archives of Electrical Engineering*, 61 (2012), No. 1, 33-46
- [13] Szeląg W., Finite element analysis of the magnetorheological fluid brake transients, *Compel*, 23 (2004), No. 6, 758-766
- [14] Wojciechowski R.M., Jędryczka C., Łukaszewicz P., Kapelski D., Analysis of high speed permanent magnet motor with powder material, *COMPEL*, 31 (2012), No. 5, 1528-1540

Autorzy:

dr inż. Mariusz Barański, Politechnika Poznańska, Instytut Elektrotechniki i Elektroniki Przemysłowej, ul. Piotrowo 3a, 60-965 Poznań, E-mail: mariusz.baranski@put.poznan.pl

dr hab. inż. Paweł Idziak, Politechnika Poznańska, Instytut Elektrotechniki i Elektroniki Przemysłowej, ul. Piotrowo 3a, 60-965 Poznań, E-mail: pawel.idziak@put.poznan.pl

dr hab. inż. Wiesław Łyskawiński, Politechnika Poznańska, Instytut Elektrotechniki i Elektroniki Przemysłowej, ul. Piotrowo 3a, 60-965 Poznań, E-mail: wieslaw.lyskawinski@put.poznan.pl

prof. dr hab. inż. Wojciech Szeląg, Politechnika Poznańska, Instytut Elektrotechniki i Elektroniki Przemysłowej, ul. Piotrowo 3a, 60-965 Poznań, E-mail: wojciech.szelag@put.poznan.pl

The correspondence address is:
e-mail: mariusz.baranski@put.poznan.pl